A DIAGNOSTIC STUDY OF THE LOCAL SOURCES AND SINKS OF MOMENTUM, KINETIC ENERGY, VORTICITY AND HEAT IN THE OBSERVED NORTHERN HEMISPHERE WINTERTIME CIRCULATION

Ngar-Cheung Lau
Geophysical Fluid Dynamics Program
Princeton University
Princeton, New Jersey, U.S.A.

1. INTRODUCTION

The quantum leap in the density and quality of the rawinsonde network during the late 1940's has facilitated the documentation of extensive data sets for empirical studies of the atmospheric general circulation. During the past three decades, many workers have endeavored to establish the essential characteristics of, and the balance requirements inherent in, the global circulation on a firm observational basis. Until quite recently, a large fraction of the investigations in this field has been concerned with the description and diagnosis of the zonally averaged circulation. Notable works along this line include the voluminous reports published by members of the Planetary Circulations Project at the Massachusetts Institute of Technology (e.g., Starr and Saltzman, 1966), the review monograph by Lorenz (1967), the review on atmospheric energetics in the wavenumber domain by Saltzman (1970), the comprehensive documentation by Oort and Rasmusson (1971), and studies by Mintz (1954), Tucker (1959), Palmen and Vuorela (1963), Holopainen (1967, 1969), among many others.

The zonally averaged formulation is attractive for a variety of reasons. By averaging various atmospheric parameters over longitude or over a spatial domain, it is feasible to present results in a compact form. Mean-flow and eddy structures can be depicted by means of zonally averaged meridional (latitude-height) cross-sections; and domain-averaged energetic cycles can be described by displaying values of various integrals in simple box diagrams. Secondly, the observational results in zonally averaged format can conveniently be compared with results given by theories and numerical models for wave-mean flow interactions, most of which being cast in the zonally averaged framework.

However, as a result of the striking inhomogeneities of the earth's orography and the distribution of continents and oceans, the nature of various forcing mechanisms exhibits a strong geographical dependence. It is evident that our understanding of the general circulation would not be complete without a clear perception of how various physical and dynamical processes vary with longitude.

The efforts to forge such a local perspective of the circulation are further motivated by the need for a deeper understanding of the variability and predictability of the regional climate; and by the opportunities offered by this approach for discovering new relationships between stationary and transient components of the circulation. Moreover, it is natural to assess the fidelity of the regional features appearing in three-dimensional general circulation model simulations by comparing model-generated statistics with observations in a local context.

Investigations on the local features of the general circulation are by no means entirely non-existent in the meteorological literature. Klein (1951) and Sawyer (1970) have examined the geographical dependence of pressure variability in the Northern Hemisphere. Crutcher (1959), Crutcher and Meserve (1970), and several members of the MIT Planetary Circulations Project (e.g., Buch, Peixoto and Obasi) have documented the hemispheric distributions of wind and transient eddy flux statistics. A comprehensive collection of contour maps of circulation statistics are found within the covers of the atlas by Newell et al. (1972, 1974). The local vorticity balance was considered in an early paper by Clapp (1956). The local heat balance was examined by Smagorinsky (1953), Clapp (1961), Brown (1964), and Geller and Avery (1978). More recently, Holopainen (1978a, 1978b, 1979) and his collaborators have diagnosed the principal components in the local balances of vorticity, kinetic energy and momentum. Plans are also underway to publish the global charts of a 15-year set of circulation statistics compiled by A.H. Oort of the Geophysical Fluid Dynamics Laboratory (GFDL).

Within the past five years, a series of observational studies of the Northern Hemisphere wintertime circulation has also been reported by J.M. Wallace of the University of Washington, M.L. Blackmon of the National Center for Atmospheric Research (NCAR) and the present author. These investigations made use of a 11-winter set of twice-daily synoptic analyses prepared on an operational basis by the U.S. National Meteorological Center (NMC). The distributions of variance and covariance statistics corresponding to different temporal and spatial scales

were considered in Blackmon (1976) and Blackmon et al. (1977). The mean flow structure and the transport properties of the transient eddies in selected longitudinal sectors were documented in Lau (1978). The local energetics of the transient disturbances and observational evidence on the life-cycle of baroclinic waves were presented in Lau (1979a). The structure of the stationary waves and the local balances of vorticity and heat were described in Lau (1979b). Lau and Wallace (1979) displayed the horizontal eddy fluxes of heat, geopotential energy, momentum, vorticity and potential vorticity in a vectorial format, and demonstrated distinct local relationships between the transient eddy fluxes and the time-mean circulation. The regional features of a wintertime simulation by a GFDL general circulation model were compared with their observed counterparts in a study by Blackmon and Lau (1980).

While it is not feasible to offer an exhaustive review of these research efforts within the scope of this report, an attempt is made here to include some of the more interesting highlights of this series of publications. After a brief description of the data base and the analysis procedures, the salient features of the stationary and transient components of the wintertime circulation are described. The nature and relative importance of the contributions by eddy transports to the local time-mean budgets of momentum, kinetic energy, vorticity and heat are then treated. Also presented are the hemispheric distributions of the local ageostrophic meridional circulations, horizontal divergence and diabatic heating, which are determined as residuals of these balances. Some remarks on several related works still in progress are made in the concluding section.

2. THE DATA SET AND ANALYSIS PROCEDURES

The data base for this series of studies consists of twice-daily NMC analyses of geopotential height, temperature and wind fields for the Northern Hemisphere at 10 pressure levels (1000, 850, 700, 500, 400, 300, 250, 200, 150 and 100 mb); as well as 6-hour forecast fields of vertical motions at the 850, 650, 500 and 350 mb levels. These data records are archived at NCAR.

The data for the analyzed fields of horizontal motion, temperature and geopotential height cover the 11 winters from 1965-66 through 1975-76. The data for vertical motion are available for the periods from 1964 to 1972, and from 1975 to 1977. The winter season is taken to be the 120-day period starting from November 15.

The procedures used in analyzing the data are summarized by the flow chart presented in Fig. 1.

After filling missing data grids by linear interpolation, the following time-filters were used to process the time series of each meteorological variable:

(a) A bandpass filter retaining fluctuations with periods between 2.5 and 6 days.

(b) A lowpass filter retaining fluctuations with periods longer than 10 days and shorter than one season.

The details of these filtering procedures have been described by Blackmon (1976).

The elements in the temporal variance and covariance matrix shown in Fig. 1 were then computed with each of the unfiltered, bandpass filtered and lowpass filtered time series. Most of the symbols in this report are used in their conventional meteorological context. The overbars denote time averages, and primes denote deviations from time averages. $\underline{z}$ represents geopotential height, $\underline{T}$ temperature, $\underline{P}$ potential vorticity, $\underline{\zeta}$ relative vorticity, $\underline{K}$ kinetic energy, $\underline{D_H}$ horizontal divergence, $\underline{\psi}$ streamfunction, $\underline{\chi}$ velocity potential and $\underline{Q}$ diabatic heating.

The three-dimensional structure of various parameters in the matrix may be examined by mapping the hemispheric distributions of the relevant fields at selected pressure levels, and by displaying partial zonal averages of these fields in the form of latitude-height cross-sections. Diagnostic studies on various aspects of the general circulation were then performed with this set of statistics.

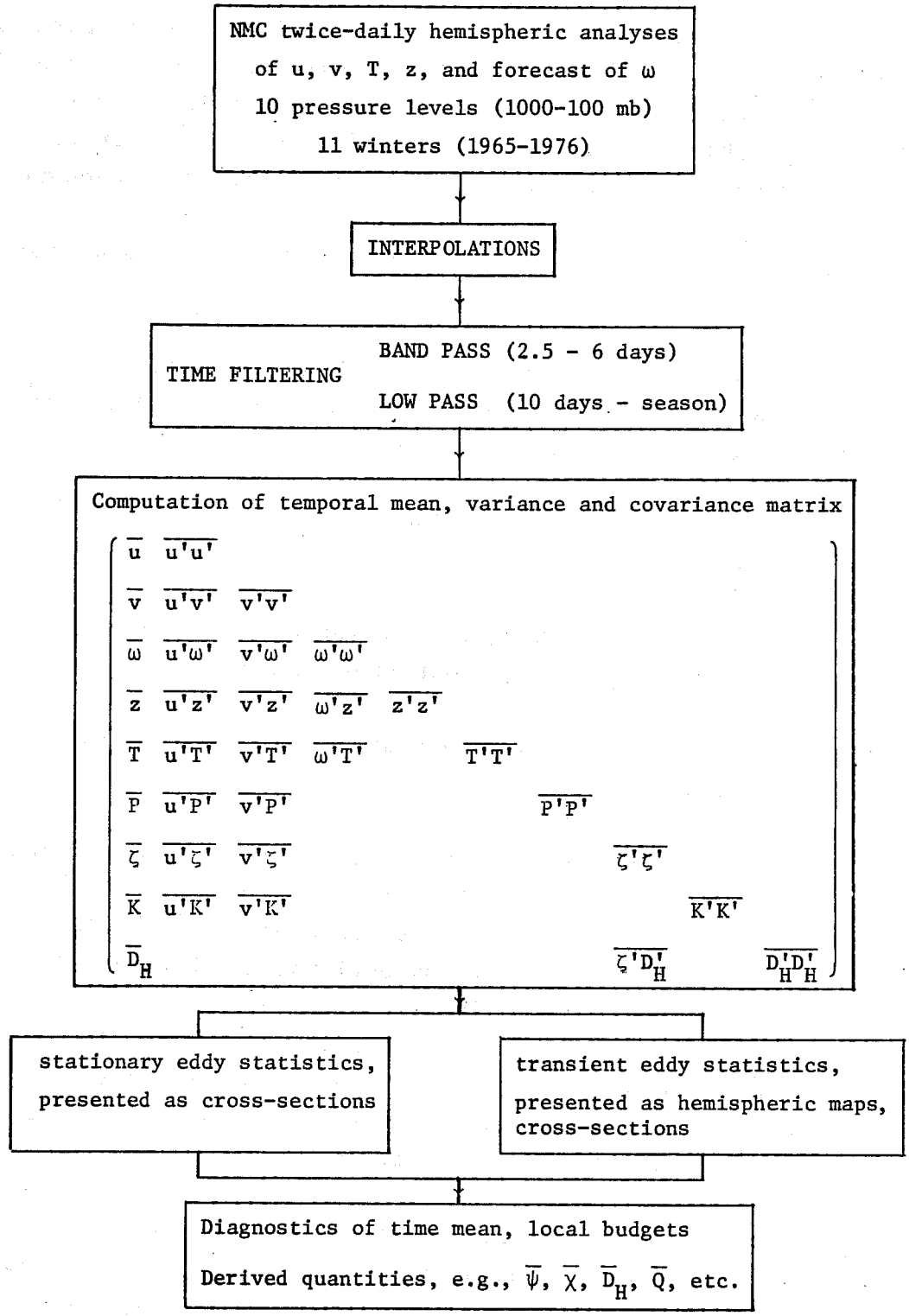

Figure 1: Flow chart of the data handling procedures.

3. ESSENTIAL FEATURES OF THE NORTHERN HEMISPHERE WINTERTIME CIRCULATION

In Fig. 2 is shown the distribution of the time-averaged geopotential height field at 300 mb. Superimposed on the same pattern are dashed contours depicting regions with strong zonal wind. The stationary circulation pattern during the winter season is characterized by the presence of prominent wave troughs (as represented by dotted lines in Fig. 2) and locally intensified jetstreams over eastern Asia, eastern North America and the Mediteranean. The southwest to northeast tilt of the stationary trough axes equatorward of 40°N, and the opposite tilt further north, infer a convergence of standing eddy momentum transports into the middle latitudes. The distinct westward tilt of the stationary wave axes with increasing height (not shown) is consistent with the observed poleward heat transports by the standing waves. The striking wave-like departures from zonal symmetry in the mean flow pattern have been attributed to stationary, geographically fixed mechanisms such as orography (Charney and Eliassen, 1949, and Bolin, 1950), diabatic heating (Smagorinsky, 1953) and mean convergence of heat and momentum transports by transient waves (Saltzman, 1962).

Embedded in the stationary flow pattern are transient phenomena which encompass a wide range of temporal and spatial scales. These transient features appear in daily synoptic charts as migratory and occluding cyclones, blocking highs and lows, etc. The structural characteristics and transport properties of these transient disturbances, as well as the geographical dependence of such properties, may be partially inferred from the three-dimensional distributions of the circulation statistics listed in Fig. 1. Features with specific scales may be isolated by subjecting time-series of the selected fields to time and space filters.

The distribution of the root-mean-squares of 500 mb geopotential height fluctuations with synoptic time scales (periods between 2.5 to 6 days) is displayed in Fig. 3. This pattern exhibits

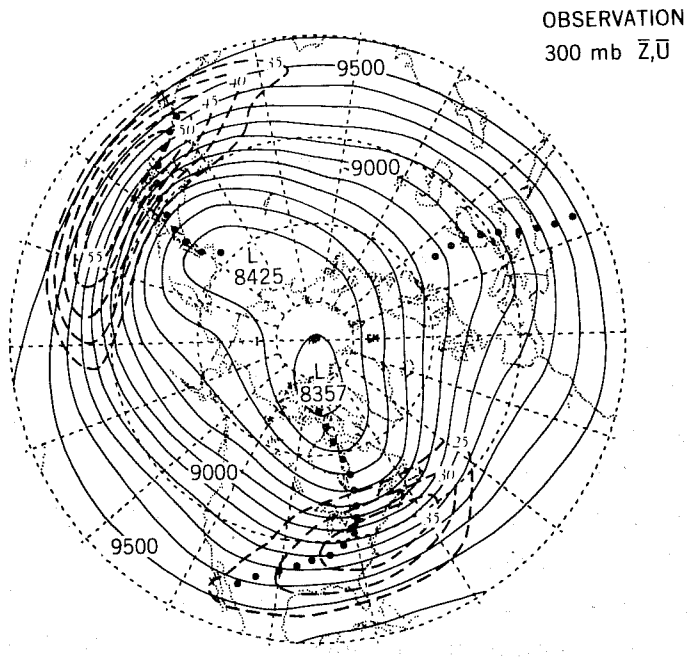

Figure 2: Distributions of the time averaged geopotential height field (solid contours, interval 100 m) and zonal wind field (dashed contours, interval 5 m s^{-1}) at 300 mb. The axes of the principal stationary troughs are depicted by dotted lines. Most figures in this report are displayed on polar stereographic projections. The meridians and latitude circles are drawn at an interval of 20°, the outermost latitude circle represents 20°N.

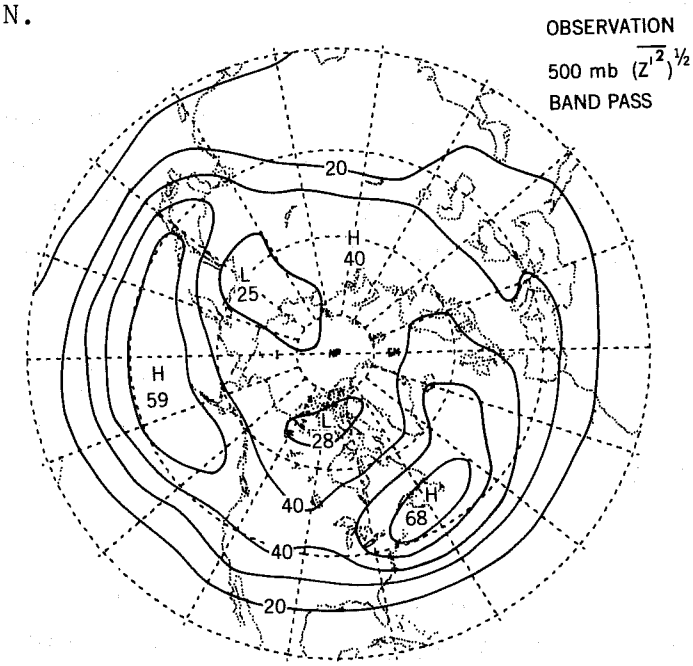

Figure 3: Distribution of the bandpass filtered root-mean-squares of the 500 mb height. Contour interval 10 m.

well-defined elongated maxima over the Pacific and the western Atlantic. The axes of these maxima correspond closely to the principal storm tracks of midlatitude cyclones in the Northern Hemisphere. These centers of action, which lie downstream and slightly poleward of the wintertime jetstreams, are characterized by strong poleward and upward eddy transports of heat, and by strong convergence of eddy transports of zonal momentum (Blackmon et al., 1977; and Lau, 1979a). The results from a cross-spectral study performed by Lau (1979a) indicate that the synoptic-scale disturbances in the cyclogenetic regions over the western oceans bear a close resemblance to developing baroclinic waves, with pronounced westward wave tilts in the vertical direction. As these disturbances evolve through their individual life cycles and move eastward along the cyclone tracks across the midlatitude oceans, they undergo noticeable structural changes. It is seen that the vertical wave tilts gradually decrease, and barotropic processes dominate. The eastern oceans and the western portion of the North American and Eurasian land masses, which correspond to the favored sites for the decay and occlusion of the travelling cyclones, are characterized by much diminished poleward and upward heat transports. These findings are consistent with the modeling results of Simmons and Hoskins (1978) on the life cycles of nonlinear baroclinic waves.

On the basis of the longitudinal variations noted above, it is possible to identify several meridional sectors in the Northern Hemisphere. These sectors are depicted in Fig. 4 and may conceptually be classified as follows:

(a) The eastern Asian (EAS) and eastern North American (ENA) sectors. These correspond to the entrance regions of the two major jetstreams, with strong vertical and lateral wind shears.

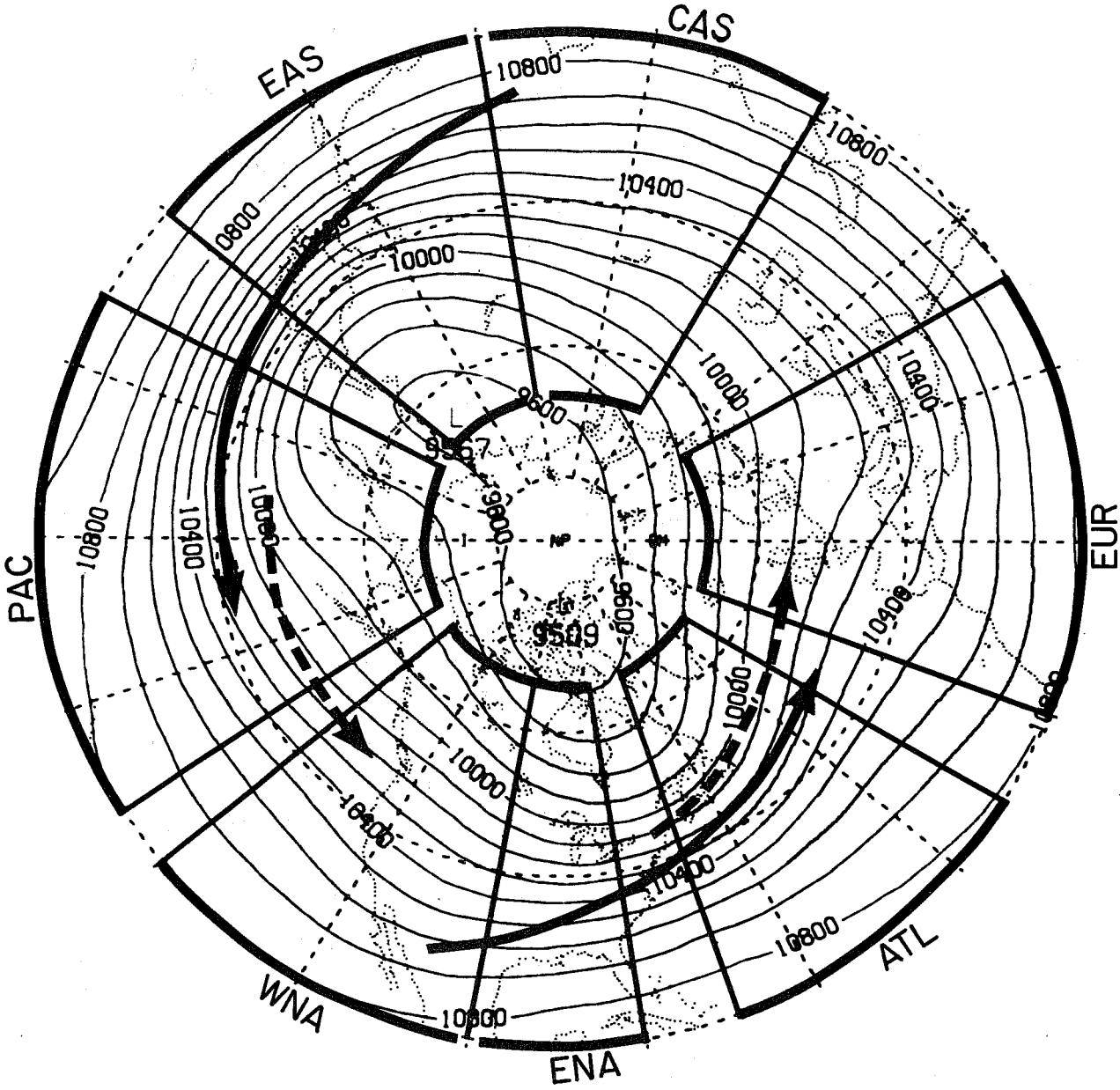

Figure 4: Distribution of the time mean geopotential height at 250 mb. Contour interval 100 m. Arrows with solid shafts denote locations of the jetstreams (see Fig. 2). Arrows with dashed shafts correspond to regions with maximum geopotential height variability in the bandpass (2.5 - 6 days) period range (see Fig. 3). Also shown are longitudinal sectors for which partial zonal averages of circulation statistics are computed.

(b) The Pacific (PAC) and Atlantic (ATL) sectors. These correspond to the exit regions of the wintertime jetstreams, and are the sites of the principal oceanic storm tracks.

(c) The western North American (WNA) and European (EUR) sectors, where the intensity of both the time mean zonal flow and the baroclinic activities are much reduced.

(d) The central Asian (CAS) sector.

Lau (1978) has delineated various aspects of the regional differences by averaging a selected set of mean, temporal variance and covariance statistics over the meridians comprising these individual sectors, and by presenting the results in the form of latitude-height cross-sections.

4. THE LOCAL BALANCES OF ZONAL MOMENTUM AND KINETIC ENERGY

By neglecting the terms involving vertical motions and friction, the local balance of zonal momentum of the time averaged flow may be expressed as

$$\underbrace{-\underset{\sim}{\overline{V}} \cdot \underset{\sim}{\nabla} \overline{u} + \frac{\tan\phi}{a} \overline{v}\,\overline{u}}_{A} \underbrace{- \underset{\sim}{\nabla} \cdot \overline{\underset{\sim}{V}'u'} + \frac{\tan\phi}{a} \overline{v'u'}}_{B} \underbrace{+ f \overline{v}_a}_{C} = 0 \qquad (1)$$

Here $\underset{\sim}{V}$ refers to the horizontal velocity vector, a the earth radius and subscript a the ageostrophic wind component.

In order to delineate the contribution of the momentum transports by transient eddies (term B) to this budget, the divergent part of the horizontal momentum flux vectors $\overline{\underset{\sim}{V}'u'} = \overline{u'u'}\,\underset{\sim}{i} + \overline{v'u'}\,\underset{\sim}{j}$ is superimposed on the coutour map of the 250 mb time averaged zonal wind (Fig. 5). A more detailed description of the decomposition of flux vectors into divergent and nondivergent parts, and the rationale for such a decomposition, are given by Lau and Wallace (1979).

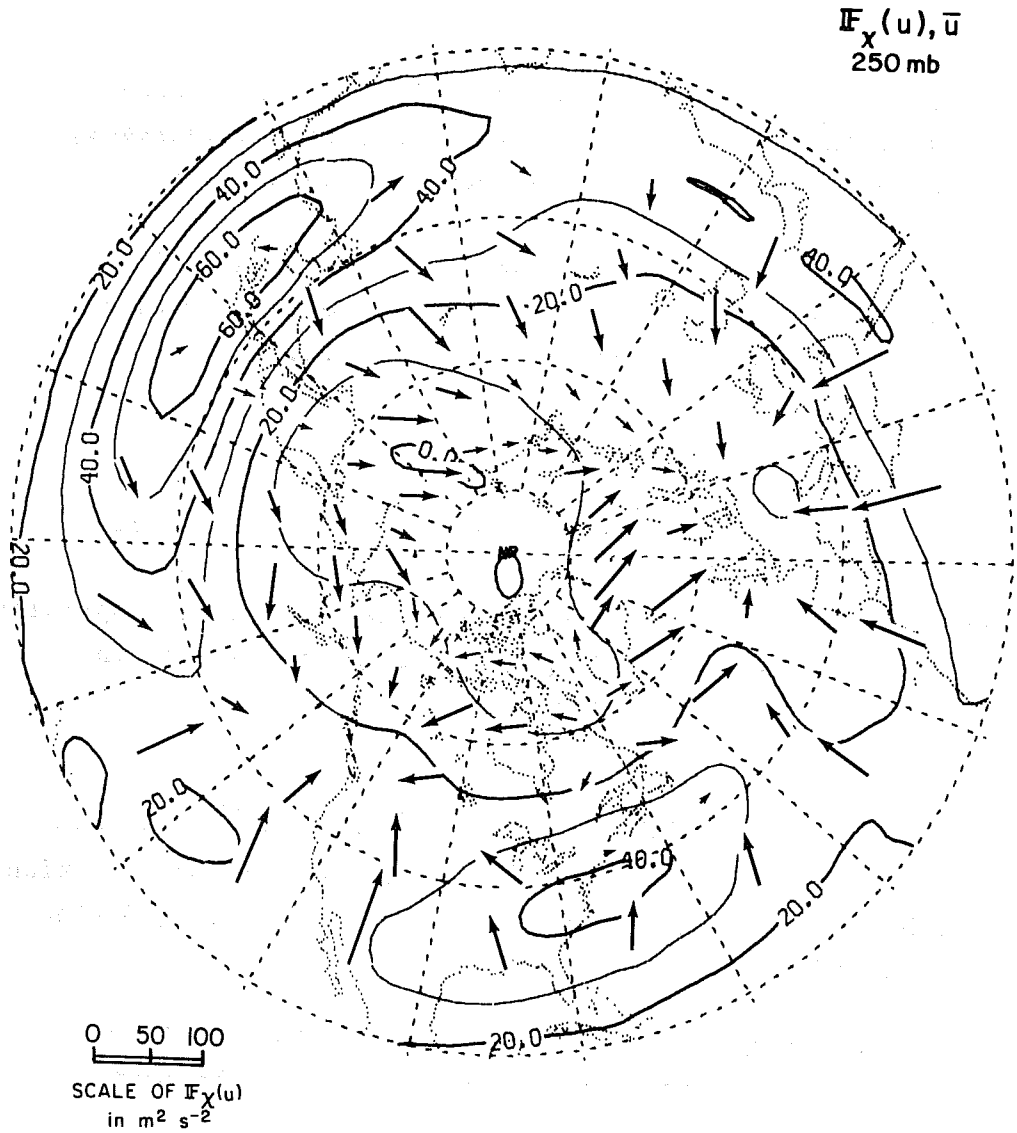

Figure 5: Vectors show the divergent part of the transient eddy flux of westerly momentum at 250 mb. The orientation of the vectors depicts the direction of the local flux. The length scale for the vectors is given in the lower left hand corner of the figure. Contours show time-averaged zonal wind at 250 mb. Contour interval 10 m s^{-1}.

The pattern is marked by a convergence of eddy momentum transports over the western parts of the major land masses (Sectors WNA and EUR in Fig. 4), where the zonal flow is relatively weak. There is indication of flux divergence over the entrance region of the Asian jetstream (Sector EAS), where the zonal flow is strong. Hence momentum transports by the transient eddies in middle latitudes act to reduce the zonal asymmetries of $\overline{u}$ associated with the standing wave pattern.

The results in Lau (1978) indicate that the advection of zonal momentum by the time mean flow (term A) is typically stronger than the eddy momentum flux convergence (term B) by a factor of 3 to 5. The direction of the ageostrophic meridional flow $\overline{v_a}$ is hence essentially determined by the sign of $-\overline{\underline{V}} \cdot \underline{\nabla} \overline{u}$. In the jet entry sectors EAS and ENA, where A<0, one would expect a poleward ageostrophic flow ($\overline{v}_a$>0) in the upper troposphere, whereas the reverse situation would prevail in the jet exit sectors PAC and ATL. In Figs. 6a and 6b are shown the meridional cross-sections of partial zonal averages of $\overline{v}_a$ in the Sectors EAS and PAC, respectively. These values of $\overline{v}_a$ were determined as residuals of the local momentum balance. Their magnitudes near the tropopause are typically 3 - 5 m s^{-1}, which are stronger than the corresponding values for the zonally averaged Ferrel circulation by a factor of about 10 (Palmen and Vuorela, 1963; and Oort and Rasmusson, 1971).

These results are consistent with the heuristic model of the wintertime jetstreams proposed by Namias and Clapp (1949) and Blackmon et al. (1977). As illustrated in the schematic sketch in Fig. 7, the poleward ageostrophic flow in the jet entrance regions (Sectors EAS and ENA) constitute the upper branches of strong thermally direct circulations. These local meridional cells extend from warm maritime regions in the subtropics, where the air is rising, to cold continental regions in the higher

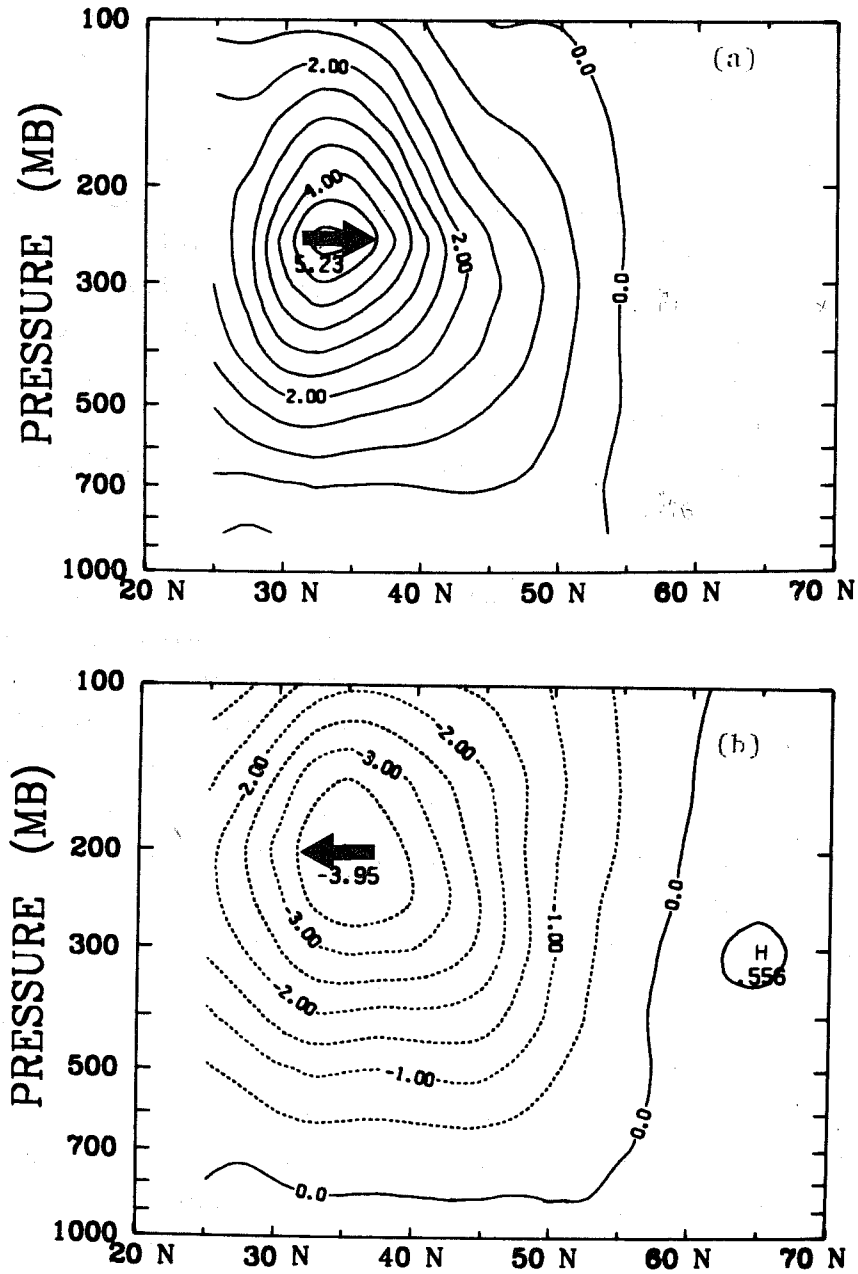

Figure 6: Meridional (latitude-height) cross sections of the sectorial averages of the meridional ageostrophic flow $\overline{v}_a$, as obtained by averaging over the meridians comprising sectors (a) EAS and (b) PAC. Refer to Fig. 4. Contour interval 0.5 m s^{-1}.

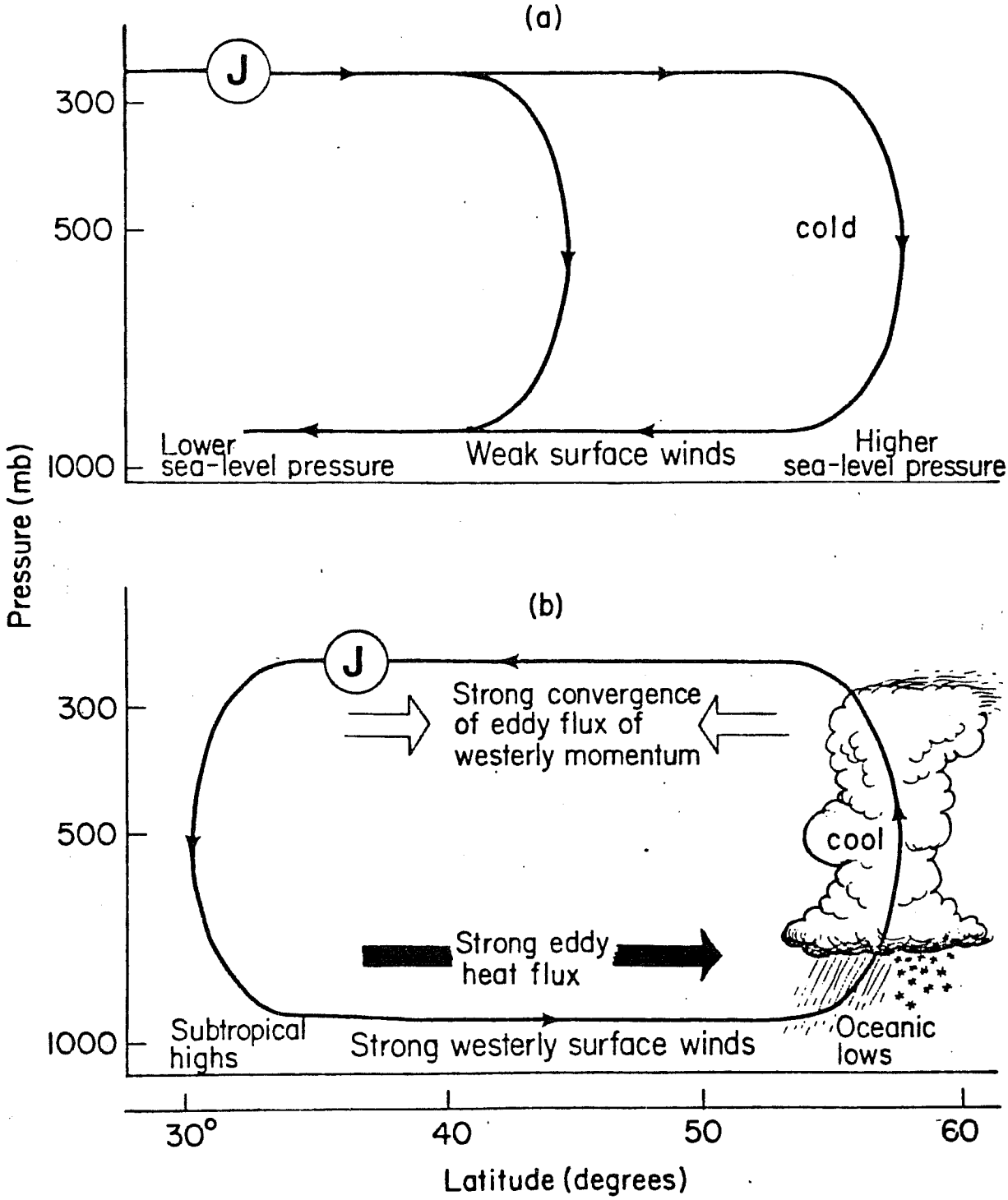

Figure 7: Schematic illustration showing relationship between the jetstreams (denoted by the letter J), the time mean circulation transverse to the jetstreams (continuous thin line with arrows), and the bandpass eddy fluxes of westerly momentum at the jetstream level (heavy white arrows) and heat at the 850 mb level (heavy black arrow), in sectors (a) EAS and ENA and (b) PAC and ATL shown in Fig. 4.

latitudes, where subsidence is taking place. Conversely, the jet exit regions (Sectors PAC and ATL) are characterized by thermally indirect circulations, with large-scale ascent over the Icelandic and Aleutian lows, and sinking over the subtropical highs.

The role of the local ageostrophic flow in the production of kinetic energy of the time averaged flow $\overline{K}_M = \frac{1}{2}(\overline{u}^2 + \overline{v}^2)$ may be demonstrated by considering the local kinetic energy balance:

$$\underbrace{-\overline{\underset{\sim}{V}} \cdot \underset{\sim}{\nabla} \overline{K}_M}_{A} \underbrace{- \overline{u}\, \underset{\sim}{\nabla} \cdot \overline{\underset{\sim}{V}'u'} - \overline{v}\, \underset{\sim}{\nabla} \cdot \overline{\underset{\sim}{V}'v'} + \frac{\tan\phi}{a}(\overline{u}\,\overline{u'v'} - \overline{v}\,\overline{v'v'})}_{B} + \underbrace{f(\overline{u}\,\overline{v}_a - \overline{v}\,\overline{u}_a)}_{C} = 0 \qquad (2)$$

The terms involving vertical motions and friction are not entered in (2). In analogy with the momentum budget, Lau (1979a) has noted that term A is locally larger than term B by a factor of 2 to 4, so that, to a good approximation, the advection of $\overline{K}_M$ by the time mean flow (term A) has to be balanced by generation or destruction of $\overline{K}_M$ due to the cross-isobar flows (terms C). The distribution of term C at 300 mb, as determined from the residual of the budget for $\overline{K}_M$, is shown in Fig. 8. The thermally direct circulations in Sectors EAS and ENA (where $\overline{v}_a > 0$, $\overline{u} > 0$) results in large local production of $\overline{K}_M$, while the equatorward ageostrophic flows accompanying the thermally indirect circulation over the oceans lead to destruction of $\overline{K}_M$.

5. THE LOCAL BALANCE OF ABSOLUTE VORTICITY

The local, time averaged balance of absolute vorticity may be expressed as

$$\underbrace{-\overline{\underset{\sim}{V}} \cdot \underset{\sim}{\nabla}(\overline{\zeta} + f)}_{A} \underbrace{- \underset{\sim}{\nabla} \cdot \overline{\underset{\sim}{V}'\zeta'}}_{B} \underbrace{- (f + \overline{\zeta})\, \overline{D}_H}_{C} = 0 \qquad (3)$$

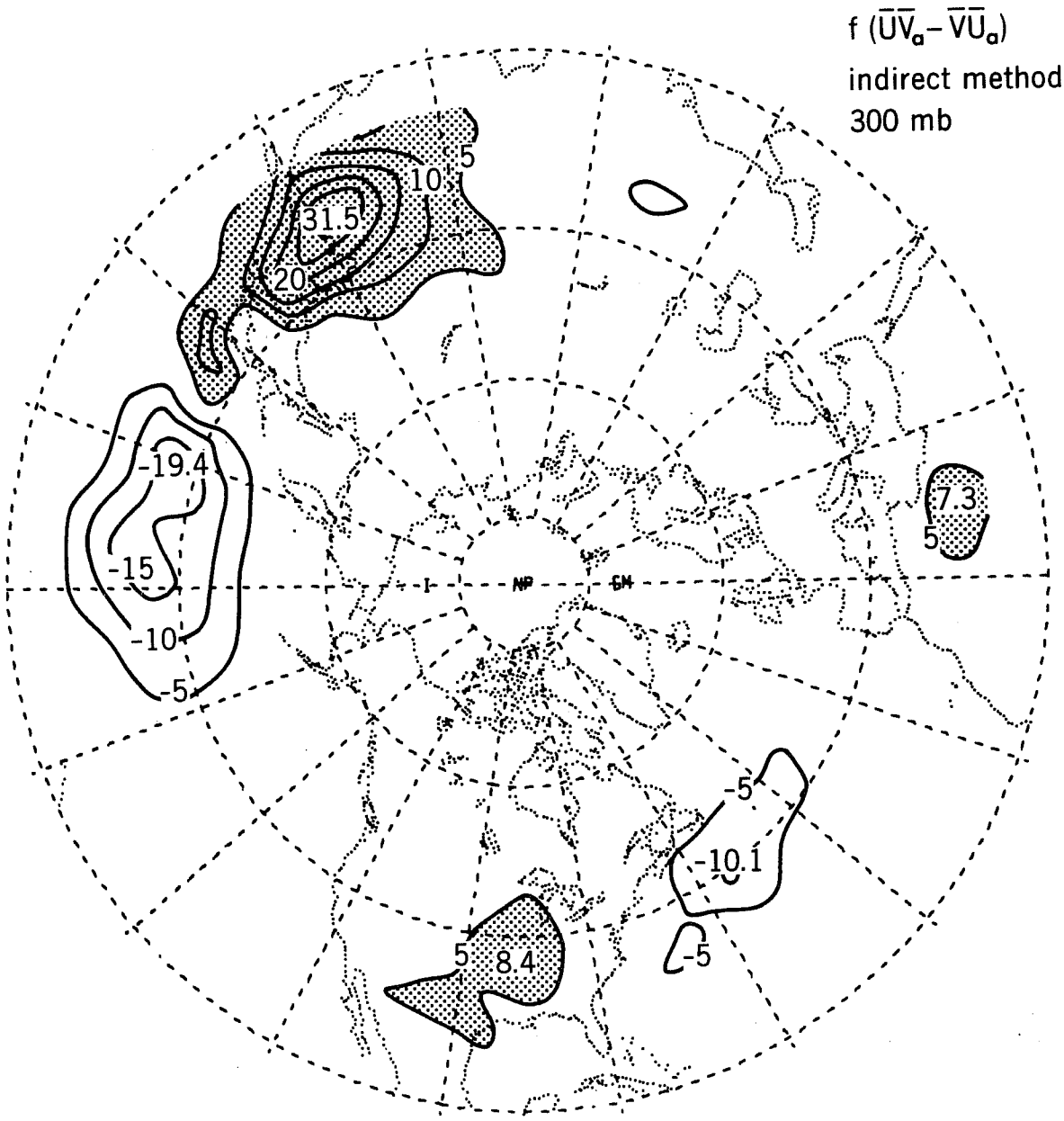

Figure 8: Distribution of the term $f(\overline{u}\ \overline{v}_a - \overline{v}\ \overline{u}_a)$ at 300 mb. Contour interval 5 x 10^{-3} m^2 s^{-3}. For the sake of clarity, the zero contour is not plotted.

The divergent part of the vector vorticity flux by the transient eddies at 300 mb $\overline{\underset{\sim}{V}'\zeta'} = \overline{u'\zeta'}\,\underset{\sim}{i} + \overline{v'\zeta'}\,\underset{\sim}{j}$ is superimposed on the contours of time-averaged 1000 mb geopotential height in Fig. 9a. The 300 mb distribution of term B itself is displayed in Fig. 9b. It is evident that the eddy transports of vorticity tend to diverge out of regions of high sea level pressure, and converge into regions of low sea level pressure. The former regions are sources of cyclonic vorticity as far as the atmosphere is concerned, since the frictional drag on the anticyclonic circulations at the earth's surface may be viewed as exerting a cyclonic torque on the atmosphere. Conversely, the Icelandic and Aleutian surface lows may be viewed as sinks of relative vorticity due to the spin down of cyclonic circulations that surround them. Hence, it appears that the transient disturbances transport vorticity from source to sink regions.

The diagnosis of the vorticity balance by Lau (1979b) suggests that terms A is typically larger than term B. It was also found that the pattern for advection of relative vorticity by the time mean flow ($-\overline{\underset{\sim}{V}} \cdot \underset{\sim}{\nabla}\,\overline{\zeta}$ in term A) tends to be negatively correlated with the pattern for the advection of planetary vorticity ($-\overline{\underset{\sim}{V}} \cdot \underset{\sim}{\nabla} f$ in term A); and that $-\overline{\underset{\sim}{V}} \cdot \underset{\sim}{\nabla}\,\overline{\zeta}$ is stronger than $-\overline{\underset{\sim}{V}} \cdot \underset{\sim}{\nabla} f$ by a factor of 3 to 4.

The 300 mb distribution of the horizontal divergence $\overline{D}_H$, as determined from the residual of this balance, is shown in Fig. 10. The maritime features of this pattern are characterized by divergence in the middle and high latitudes, and by convergence over the subtropics. The distribution over land suggests the influence of the underlying topography, with divergence to the west of the Himalyas and the Canadian Rockies, and convergence to the east. In Lau (1979b), this diagnosed divergence field was utilized to compute the velocity potential and the mean vertical motion fields.

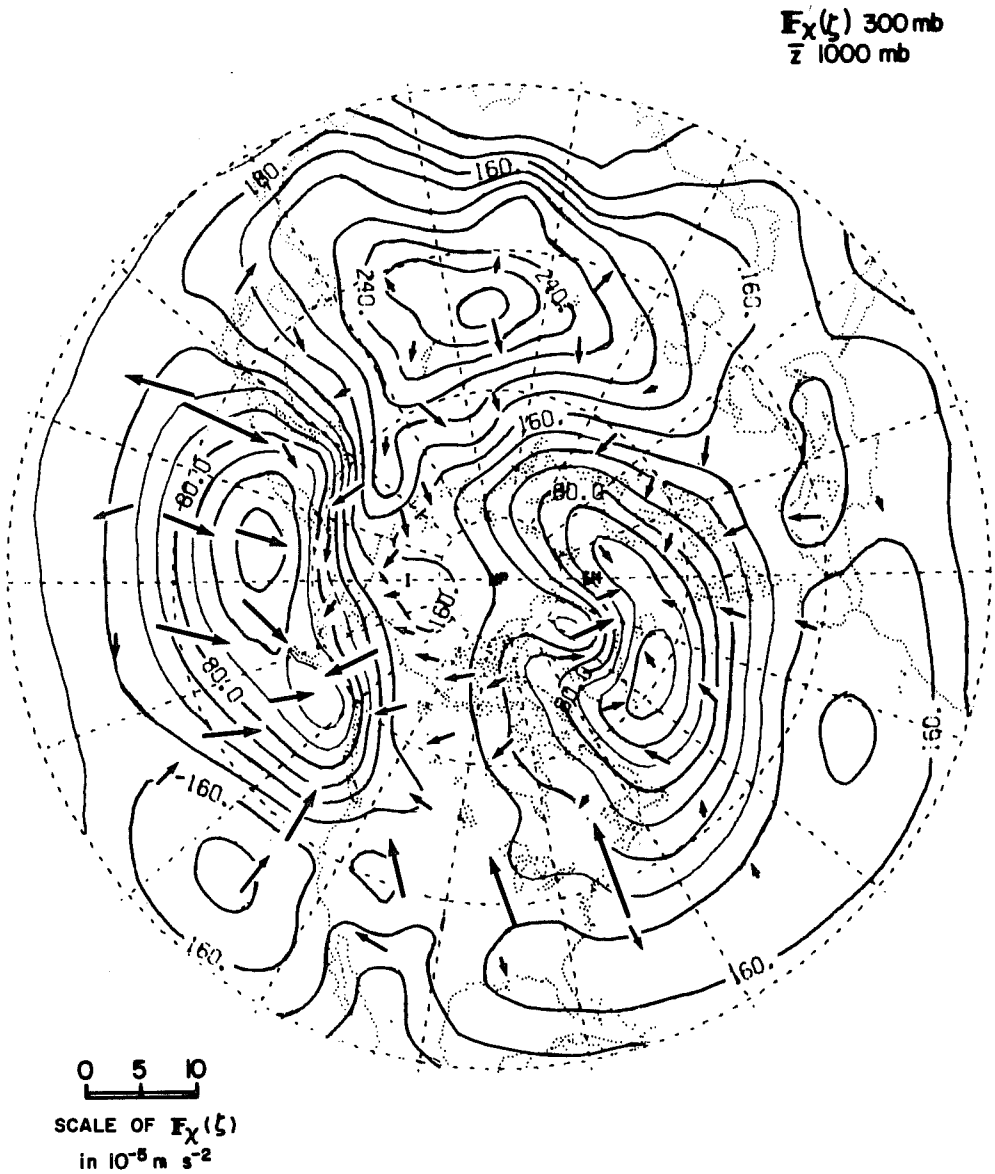

Figure 9a: Vectors show divergent part of the transient eddy flux of relative vorticity at 300 mb. Contours show time averaged sea level pressure field, expressed in terms of height of the 1000 mb surface. Contour interval, 20 m. Also refer to caption of Fig. 5.

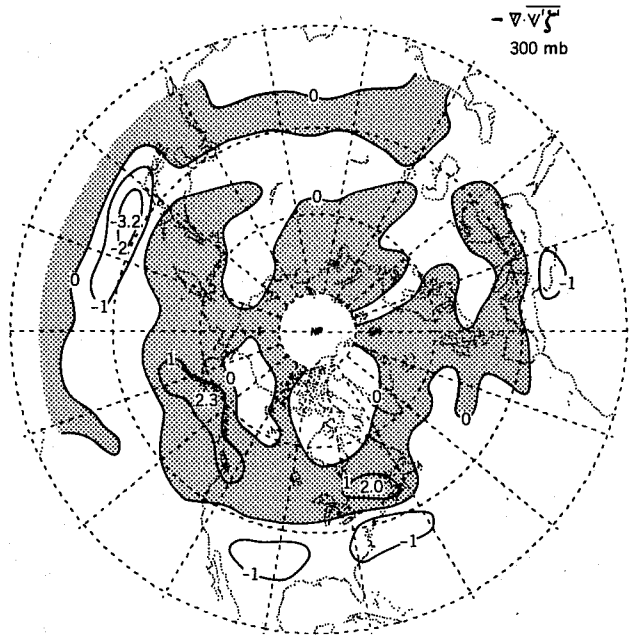

Figure 9b: Distribution of $-\underset{\sim}{\nabla} \cdot \overline{\underset{\sim}{V}'\zeta'}$ at 300 mb. Contour interval 1 x 10^{-10} s^{-2}.

It is interesting to compare the pattern of the horizontal divergence field in Fig. 10 with that of the time-averaged 500 mb pressure velocity field based on the 6-hour forecasts produced by the NMC numerical prediction models, shown in Fig. 11. There is on the whole a good correspondence between upper level flow divergence (convergence) and upward (downward) motions at 500 mb. These results also lend credence to the postulated existence of thermally direct circulations over the jet entry regions, and thermally indirect circulations over the jet exit regions.

6. THE LOCAL BALANCE OF HEAT

The time averaged, local balance of heat may be expressed as:

$$\underbrace{-\overline{\underset{\sim}{V}} \cdot \underset{\sim}{\nabla}\,\overline{T} + \sigma\,\overline{\omega}}_{A} \underbrace{- \underset{\sim}{\nabla} \cdot \overline{\underset{\sim}{V}'T'} - \frac{\partial}{\partial p}\,\overline{\omega'T'} + \frac{R}{pc_p}\,\overline{\omega'T'}}_{B} + \underbrace{\overline{Q}}_{C} = 0 \qquad (4)$$

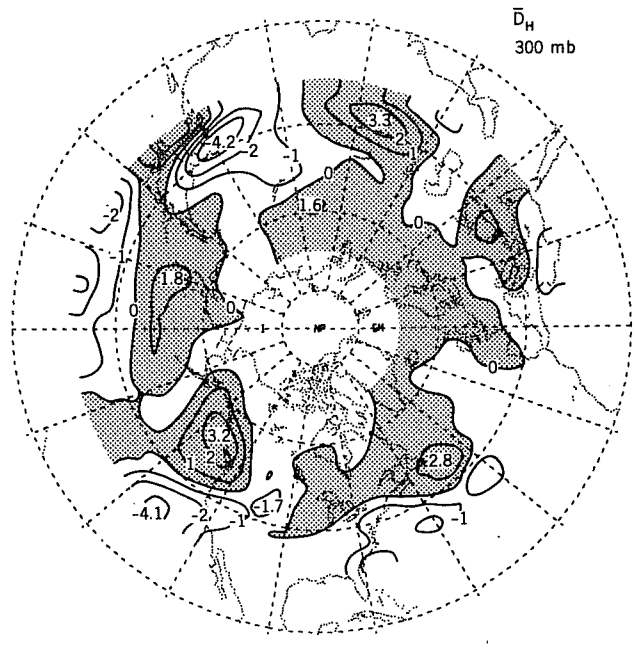

Figure 10: Distribution of the time averaged divergence $\bar{D}_H$ at 300 mb. Contour interval 1 x 10^{-6} s^{-1}.

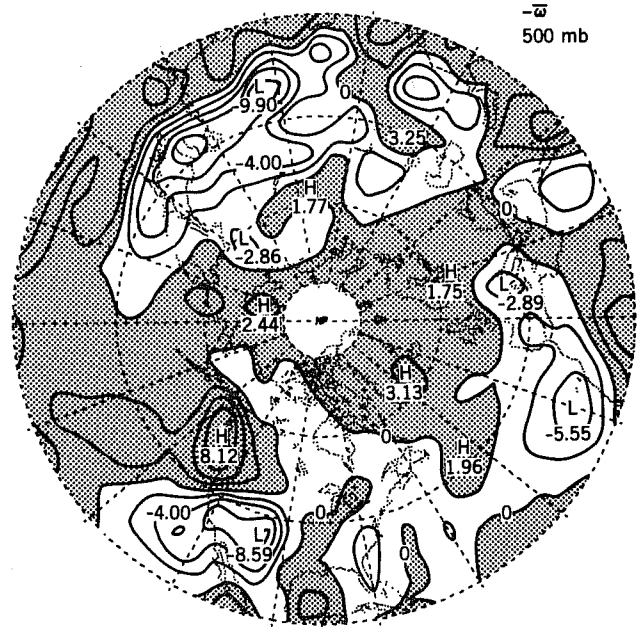

Figure 11: Distribution of the time averaged 500 mb pressure velocity, $-\bar{\omega}$, based on 6-hour forecasts of the NMC models. Contour interval 2 x 10^{-4} mb s^{-1}. Shading indicates rising motion.

The horizontal transport of heat by transient eddies at 850 mb $\overline{\underset{\sim}{V}'T'} = \overline{u'T'}\,\underset{\sim}{i} + \overline{v'T'}\,\underset{\sim}{j}$ is depicted in a vectorial format in Fig. 12a. The contours of the time averaged 850 mb temperature field are superimposed on the same map. The distribution of the convergence of horizontal eddy heat transport $-\underset{\sim}{\nabla} \cdot \overline{\underset{\sim}{V}'T'}$ at 700 mb (which is similar to that at 850 mb) is shown in Fig. 12b. The fluxes show a strong tendency to be directed down the local temperature gradient from higher towards lower temperatures. Hence the transient eddies are not only acting to reduce the zonally averaged meridional temperature gradient, but also the east-west temperature gradients associated with the standing wave pattern. The close correspondence between the positive (negative) departures of $\overline{T}$ from zonal symmetry and divergence (convergence) of eddy heat transport further suggests that the transient disturbances tend to destroy the wave-like structure of the stationary temperature field. The time-scale of this dissipative mechanism, as given by the ratio of the wave amplitude of the stationary temperature field to that of $-\underset{\sim}{\nabla} \cdot \overline{\underset{\sim}{V}'T'}$, is of the order of several days.

In Fig. 13 is shown the distribution of the diabatic heating field $\overline{Q}$ at 700 mb, which is determined as a residual of the heat balance. This pattern is indicative of the primary importance of geographically-fixed influences such as ocean currents and sea-land contrast. The heating over the western oceans is probably associated with the transfer of sensible and latent heat from the warm Kuroshio and Gulf Stream currents underlying these regions. The prevalent cooling over continental regions is essentially a result of sensible heat loss to the ground.

7. CONCLUDING REMARKS

Since the documentation of three-dimensional data sets for local budget studies is still somewhat hindered by the existence of spatial data gaps over the oceans and other remote regions, it is useful to perform detailed intercomparisons of circulation statistics derived form independent analysis procedures. Such a project has recently been undertaken by A.H. Oort and the present author. The data sets used in this study include:

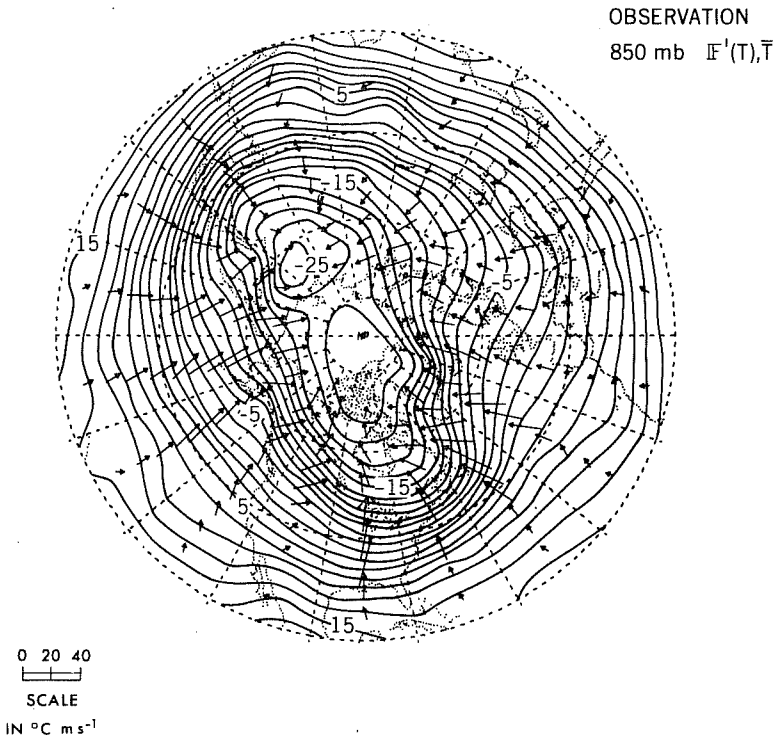

Figure 12a: Vectors show tranient eddy heat flux at the 850 mb level. Contours show time mean 850 mb temperature. Contour interval 2 °C. Also refer to caption of Fig. 5.

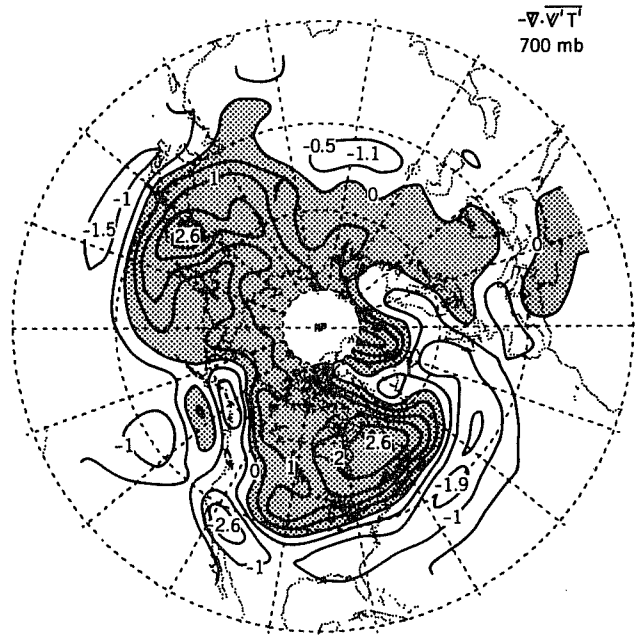

Figure 12b: Distribution of $-\underset{\sim}{\nabla} \cdot \overline{\underset{\sim}{V}'T'}$ at 700 mb. Contour interval 0.5 °C day^{-1}.

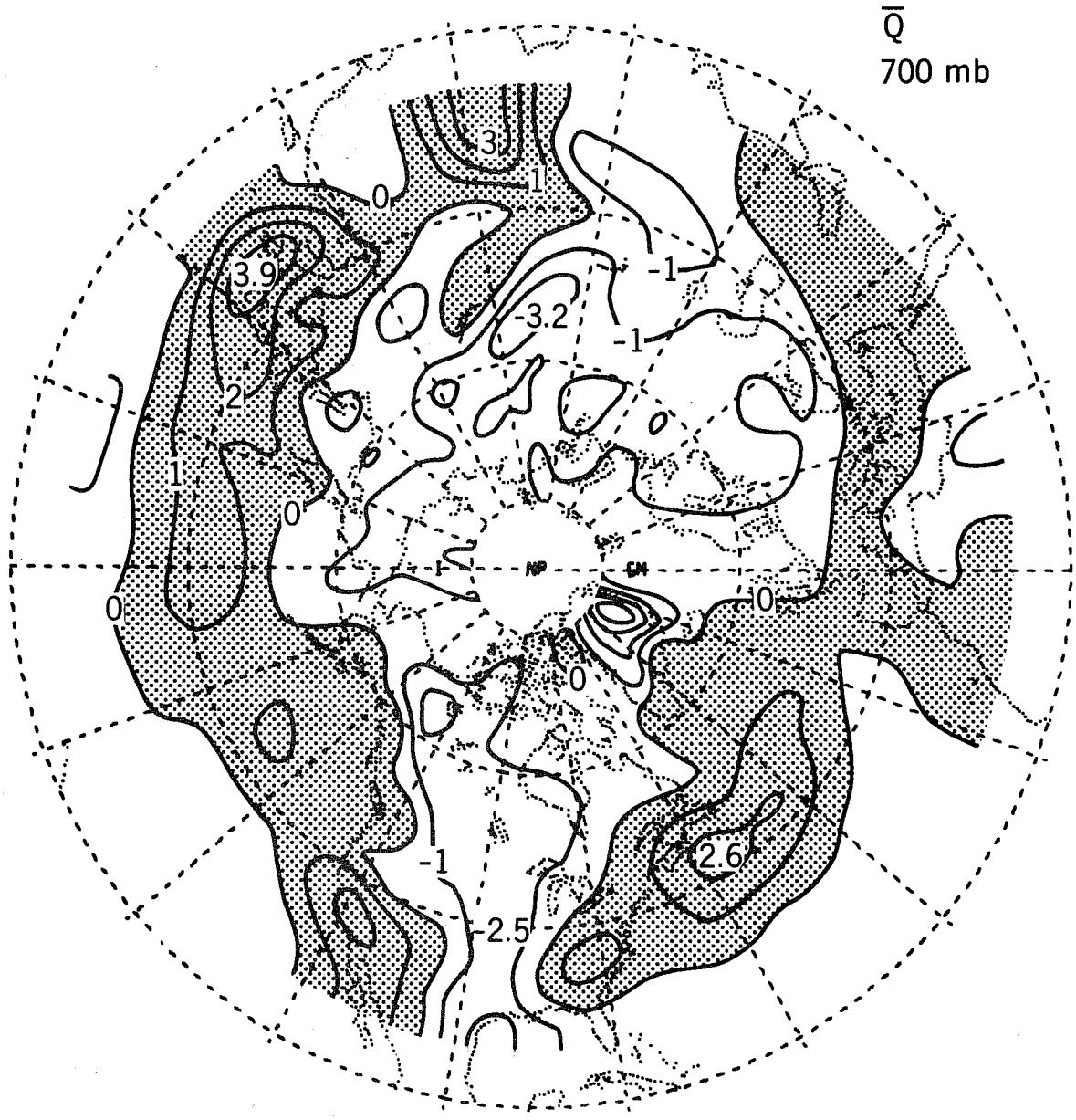

Figure 13: Distribution of diabatic heating rate $\overline{Q}$ at 700 mb. Contour interval 1 °C day^{-1}.

(a) The GFDL General Circulation Library, which is composed of objective horizontal analyses of monthly circulation statistics evaluated at individual rawinsonde stations. Refer to Oort and Rasmusson (1971) for details.

(b) The NMC set used in the series of studies described in this report. The statistics were compiled by making use of the gridded data for twice-daily synoptic analyses.

(c) The Monthly Climatic Data for selected rawinsonde stations, as documented by the World Meteorological Organization in cooperation with the U.S. National Climatic Center.

The results of this study indicate that there is a close agreement between the three data sets over regions with a dense network of observing stations. Although larger systematic differences between the GFDL and NMC data sets are found over the data-sparse regions, the qualitative features of some of the most essential findings reported here (e.g., the displacement of the storm tracks relative to the jetstreams, Fig. 4; the tendency for convergence of eddy momentum flux into regions of weak zonal wind, Fig. 5, and for eddy heat transports to be directed down the local temperature gradient, Fig. 12a) show up in both data sets. With the advent of more sophisticated observing systems and data assimilation schemes, such as those being implemented in the Global Weather Experiment, it is anticipated that the problems related to data deficiencies will eventually be overcome to a considerable extent.

G.H. White of the University of Washington has compiled a parallel set of NMC statistics for the summer season, and is presently examining the contrast between the Northern Hemisphere circulation during the summer and winter seasons. The statistics for both seasons will be published in the form of a climate atlas, and the data summaries will be included in the NCAR archive tape library.

The Level III-b data sets for the Global Weather Experiment, to be assembled independently by ECMWF and GFDL, offer an unique opportunity for a comprehensive investigation of the circulation systems in all parts of the globe. These data sets will offer an adequate description of the three-dimensional structure of the tropical and Southern Hemisphere circulations for the first time. The diagnoses of these data sets will undoubtedly yield fresh insights into such problems as tropics-extratropics interactions, interhemispheric exchanges, and the role of the diurnal cycle in the global circulation.

REFERENCES

Blackmon, M.L., 1976: A climatological spectral study of the 500 mb geopotential height of the Northern Hemisphere. J. Atmos. Sci., 33, 1607-1623.

Blackmon, M.L., J.M. Wallace, N.C. Lau and S.L. Mullen, 1977: An observational study of the Northern Hemisphere wintertime circulation. J. Atmos. Sci., 34, 1040-1053.

Blackmon, M.L., and N.C. Lau, 1980: Regional characteristics of the Northern Hemisphere wintertime circulation: A comparison of the simulation by a GFDL general circulation model with observations. J. Atmos. Sci., 37, 497-514.

Bolin, B., 1950: On the influence of the earth's orography on the general character of the westerlies. Tellus, 2, 184-195.

Brown, J.A., 1964: A diagnostic study of tropospheric diabatic heating and the generation of available potential energy. Tellus, 16, 371-388.

Charney, J.G., and A. Eliassen, 1949: A numerical method for predicting the perturbations of the middle latitude westerlies. Tellus, 1, 38-54.

Clapp, P.F., 1956: Some considerations involved in preparing long range forecasts by numerical methods. J. Meteor., 13, 341-350.

Clapp, P.F., 1961: Normal heat sources and sinks in the lower troposphere in winter. Mon. Wea. Rev., 89, 147-162.

Crutcher, H.L., 1959: Upper wind statistics charts of the Northern Hemisphere. Vol. 1 and 2, NAVAER 50-1C-535, Office of the Chief of Naval Operations, Washington, D.C.

Crutcher, H.L., and J.M. Meserve, 1970: Selected level heights, temperatures and dew points for the Northern Hemisphere. NAVAIR 50-1C-52, for sale by the Superintendent of Documents, U.S. Govt. Printing Office, Washington D.C.

Geller, M.A., and S.K. Avery, 1978: Northern Hemisphere distributions of diabatic heating in the troposphere derived from general circulation data. Mon. Wea. Rev., 106, 629-636.

Holopainen, E.O., 1967: On the mean meridional circulation and the flux of angular momentum over the Northern Hemisphere. Tellus, 19, 1-13.

Holopainen, E.O., 1969: On the maintenance of the atmosphere's kinetic energy over the Northern Hemisphere in winter. Pure and Applied Geophysics, 77, 104-121.

Holopainen, E.O., 1978a: On the dynamic forcing of the long term mean flow by the large scale Reynolds stresses in the atmosphere. J. Atmos. Sci., 35, 1596-1604.

Holopainen, E.O., 1978b: A diagnostic study of the kinetic energy balance of the long-term mean flow and the associated transient fluctuations in the atmosphere. Geophysica, 15, 125-145.

Holopainen, E.O., 1979: A diagnostic study of the long-term budget of momentum of atmospheric large scale motion over the British Isles. Quart. J. Roy. Meteor. Soc., 105, 859-871.

Klein, W.H., 1951: A hemispheric study of daily pressure variability at sea level and aloft. J. Meteor., 8, 332-346.

Lau, N.C., 1978: On the three-dimensional structure of the observed transient eddy statistics of the Northern Hemisphere wintertime circulation. J. Atmos. Sci., 35, 1900-1923.

Lau, N.C., 1979a: The structure and energetics of transient disturbances in the Northern Hemisphere wintertime circulation. J. Atmos. Sci., 36, 982-995.

Lau, N.C., 1979b: The observed structure of tropospheric stationary waves and the local balances of vorticity and heat. J. Atmos. Sci., 36, 996-1016.

Lau, N.C., and J.M. Wallace, 1979: On the distribution of horizonatal transports by transient eddies in the Northern Hemisphere wintertime circulation. J. Atmos. Sci., 36, 1844-1861.

Lorenz, E.N., 1967: The nature and theory of the general circulation of the atmosphere. World Meteorological Organization, Geneva, 161 pp.

Mintz, Y., 1954: The observed zonal circulation of the atmosphere. Bull. Amer. Meteor. Soc., 35, 208-214.

Namias, J., and P.F. Clapp, 1949: Confluence theory of high tropospheric jet stream. J. Meteor., 6, 330-336.

Newell, R.E., J. W. Kidson, D.G, Vincent and G.T. Boer, 1972 and 1974: The general circulation of the tropical atmosphere, Volumes I and II. The M.I.T. Press, Cambridge, Mass., 258 and 370 pp.

Oort, A.H., and E.M. Rasmusson, 1971: Atmospheric circulation statistics. NOAA Prof. Pap. 5, U.S. Dept. of Commerce, 323 pp.

Palmen, E., and L.A. Vuorela, 1963: On the mean meridional circulations in the Northern Hemisphere during the winter season. Quart. J. Roy. Meteor. Soc., 89, 131-138.

Saltzman, B., 1962: Empirical forcing functions for the large-scale mean disturbances in the atmosphere. Geofisica Pura e Applicata, 52, 173-188.

Saltzman, B., 1970: Large-scale atmospheric energetics in the wave-number domain. Rev. Geophys. Space Phys., 8, 289-302.

Sawyer, J.S., 1970: Observational characteristics of atmospheric fluctuations with a time scale of a month. Quart. J. Roy. Meteor. Soc., 96, 610-625.

Simmons, A.J., and B.J. Hoskins, 1978: The life cycles of some nonlinear baroclinic waves. J. Atmos. Sci., 35, 414-432.

Smagorinsky, J., 1953: The dynamical influence of large-scale heat sources and sinks on the quasi-stationary mean motions of the atmosphere. Quart. J. Roy. Meteor. Soc., 79, 343-366.

Starr, V.P., and B. Saltzman, ed., 1966: Observational Studies of the Atmospheric General Circulation. Scientific Report #2. Planetary Circulation Project, M.I.T., 700 pp.

Tucker, G.B., 1959: Mean meridional circulations in the atmosphere. Quart. J. Roy. Meteor. Soc., 85, 209-224.